

## Raman spectroscopy of localized vibrational modes from carbon and carbon-hydrogen pairs in heavily carbon-doped GaAs epitaxial layers

J. Wagner, M. Maier, Th. Lauterbach, and K. H. Bachem

*Fraunhofer-Institut für Angewandte Festkörperphysik, Tullastrasse 72, D-7800 Freiburg,  
Federal Republic of Germany*

A. Fischer and K. Ploog

*Max-Planck-Institut für Festkörperforschung, Heisenbergstrasse 1, D-7000 Stuttgart 80,  
Federal Republic of Germany*

G. Mörsch and M. Kamp

*Institut für Schichten und Ionentechnik, Forschungszentrum Jülich, P.O. Box 1913, D-5170 Jülich,  
Federal Republic of Germany*

(Received 25 November 1991)

Heavily carbon-doped GaAs layers have been studied by Raman spectroscopy of localized vibrational modes. Films grown by three different epitaxial techniques—namely molecular-beam epitaxy, metalorganic vapor-phase epitaxy (MOVPE), and metalorganic molecular-beam epitaxy—have been examined. Samples grown by MOVPE show—besides scattering by the  $^{12}\text{C}_{\text{As}}$  local vibrational mode near  $583\text{ cm}^{-1}$ , which is observed for all three growth techniques—two additional lines at  $452$  and  $2640\text{ cm}^{-1}$  for carbon concentrations  $> 5 \times 10^{19}\text{ cm}^{-3}$ . These lines are assigned to the stretch mode of  $^{12}\text{C}_{\text{As}}\text{-H}$  pairs ( $2640\text{ cm}^{-1}$ ) and to a carbon mode of these pairs ( $452\text{ cm}^{-1}$ ). The analysis of polarization selection rules indicates that the  $452\text{-cm}^{-1}$  mode is longitudinal ( $A_1$  symmetry). It shows a pronounced resonance enhancement in scattering strength for incident-photon energies in resonance with the GaAs  $E_1$  band-gap energy.

### I. INTRODUCTION

Carbon doping of GaAs epitaxial layers has attracted considerable interest for application in the preparation of highly conducting  $p$ -type material.<sup>1–5</sup> Carbon is known to be probably the best acceptor-doping element in the GaAs/ $\text{Al}_x\text{Ga}_{1-x}\text{As}$  material system. High doping levels with reasonably low compensation ratios and low diffusion constants have been reported for this acceptor. Hole concentrations exceeding  $10^{21}\text{ cm}^{-3}$  have been achieved in layers grown by, e.g., metalorganic molecular-beam epitaxy (MOMBE).<sup>4</sup> For these high concentrations in some cases, however, the doping efficiency was found to be only about 40%.<sup>5</sup> This implies that a substantial fraction of the carbon impurities can be either electrically inactive or compensated by donors. It has been speculated that some of the carbon atoms may act either as interstitial donors or as substitutional donors with the carbon impurity being incorporated on a Ga lattice site.

Local-vibrational-mode (LVM) absorption spectroscopy, which gives direct information about the lattice location of the impurities,<sup>6</sup> has been used to study the incorporation of carbon in epitaxial GaAs layers.<sup>7–9</sup> The observation of carbon-hydrogen nearest-neighbor pairs, both in intentionally hydrogenated material<sup>8</sup> as well as in as-grown films prepared by MOMBE (Ref. 7) and by metalorganic vapor-phase epitaxy (MOVPE),<sup>9</sup> makes carbon-doped GaAs layers an interesting material for the study of acceptor-hydrogen complexes. The presence of

such electrical neutral complexes in layers grown from hydrogen-containing precursors may account at least for part of the reduced doping efficiency for the high dopant concentration mentioned above.<sup>5</sup>

To study the impurity-induced LVM of Si and Be in GaAs, in addition to infrared-absorption spectroscopy, Raman spectroscopy has also been used successfully.<sup>10</sup> However, there is only one preliminary report on the Raman-spectroscopic study of carbon LVM in carbon-doped GaAs layers.<sup>11</sup> In the present work a variety of heavily carbon-doped GaAs layers prepared by different growth techniques have been investigated by LVM Raman spectroscopy. The strength of the carbon acceptor ( $\text{C}_{\text{As}}$ ) LVM has been correlated with the carbon concentration. Heavily-carbon-doped layers grown by MOVPE, which contain carbon-hydrogen complexes already in the as-grown state, are found to show Raman scattering by the stretch mode of the  $^{12}\text{C}_{\text{As}}\text{-H}$  pair, as well as by the longitudinal carbon mode of that pair.

### II. EXPERIMENT

Epitaxial layers of GaAs highly doped with carbon were grown by solid-source molecular-beam epitaxy (MBE), MOVPE, and MOMBE, respectively. For MBE growth a newly developed carbon effusion cell based on a resistively heated graphite filament was used as the carbon source.<sup>12</sup> The substrate temperature was  $560^\circ\text{C}$  for sample 1 in Table I and  $500^\circ\text{C}$  for samples 2 and 3. MOVPE growth was performed using trimethylgallium

TABLE I. Carbon concentrations  $[C]$  measured by SIMS and free-hole concentration  $p$  measured by Hall effect for the samples used in the present study. The accuracy of the SIMS data is  $\pm 20\%$  and that of the Hall-effect data is  $\pm 10\%$ .

Sample No.	Growth technique	$[C]$ ( $\text{cm}^{-3}$ )	$p$ ( $\text{cm}^{-3}$ )
1	MBE	$3.5 \times 10^{19}$	$8 \times 10^{18}$
2	MBE	$1.2 \times 10^{20}$	$1.4 \times 10^{19}$
3	MBE	$2.5 \times 10^{20}$	$2.7 \times 10^{19}$
4	MOMBE	$2.4 \times 10^{19}$	$3 \times 10^{19}$
5	MOMBE	$8.4 \times 10^{19}$	$1 \times 10^{20}$
6	MOMBE	$1.5 \times 10^{20}$	$1.1 \times 10^{20}$
7	MOVPE	$1.2 \times 10^{19}$	$9.5 \times 10^{18}$
8	MOVPE	$6 \times 10^{19}$	$5.6 \times 10^{19}$
9	MOVPE	$1.8 \times 10^{20}$	$1.2 \times 10^{20}$

(TMGa) and trimethylarsine.<sup>13</sup> With this group-V source material, carbon concentrations in the range of  $10^{20} \text{ cm}^{-3}$  can be achieved.<sup>13</sup> A specific feature of this procedure is that both GaAs growth and carbon doping are simultaneously controlled by the choice of MOVPE-growth parameters. The samples used in the present study were grown at a substrate temperature of  $540^\circ\text{C}$  (sample 9) and  $585^\circ\text{C}$  (samples 7 and 8), where sample 7 was placed in the MOVPE reactor further downstream than sample 8. The pressure in the reactor was 100 mbar in all cases. The MOMBE samples were grown from TMGa and pre-cracked arsine. Both precursors were used by direct distillation. The growth temperature was kept constant at  $540^\circ\text{C}$ . The carbon concentration was varied by means of the group-V- to group-III-element ratio, which was in the range 0.25–1.

The GaAs layers investigated were doped with carbon concentrations ranging from  $1.2 \times 10^{19}$  to  $2.5 \times 10^{20} \text{ cm}^{-3}$ . The layer thicknesses varied between 0.8 and 3.5  $\mu\text{m}$ . The films grown were analyzed by secondary-ion-mass spectroscopy (SIMS), to assess the total carbon concentration  $[C]$ , and by room-temperature Hall-effect measurements to determine the free-hole concentration  $p$ . The results are listed in Table I.

The Raman experiments were performed in the back-scattering geometry from a (100) surface of the as-grown samples. The spectra were excited either with the 3.00- or 3.05-eV line of a Kr-ion laser or with the 2.71-eV line of an Ar-ion laser. The laser light incident on the sample at a power of  $\approx 150$ – $200$  mW was focused to a spot  $\approx 50 \mu\text{m}$  in diameter. For crystalline GaAs, the probing depth  $1/(2\alpha)$ , where  $\alpha$  denotes the absorption coefficient, is  $\approx 10$  and  $\approx 20$  nm for the highest and lowest photon energy used, respectively.<sup>14</sup> The samples were cooled to 77 K. The scattered light was filtered and dispersed in a triple monochromator and detected with an intensified silicon-diode array.

### III. RESULTS AND DISCUSSION

A sequence of Raman spectra showing the  $^{12}\text{C}_{\text{As}}$  LVM is displayed in Fig. 1. The spectra were recorded from MBE-grown samples doped with carbon to a concentra-

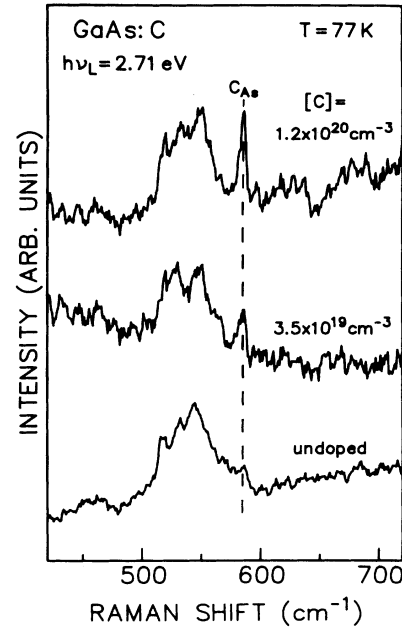


FIG. 1. Low-temperature Raman spectra of MBE-grown GaAs:C with different dopant concentrations (samples 1 and 2 in Table I) given in the figure. The spectra were excited at 2.71 eV. The spectral resolution was set to  $4 \text{ cm}^{-1}$ .

tion of  $3.5 \times 10^{19} \text{ cm}^{-3}$  (sample 1) and  $1.2 \times 10^{20} \text{ cm}^{-3}$  (sample 2), respectively. For reference purposes the spectrum of undoped GaAs is also displayed. All spectra were excited at 2.71 eV, which is below the  $E_1$ -band-gap resonance of GaAs. The incident light was polarized parallel to a [100] crystallographic direction. The scattered light was not intentionally analyzed for its polarization, but the throughput of the spectrometer was higher for scattered light with polarization perpendicular to that of the incident light. Thus, Raman scattering described by Raman tensors with  $\Gamma_{15}$  and  $\Gamma_{25}$  symmetry<sup>15</sup> is preferentially observed.

Besides the  $\text{C}_{\text{As}}$  LVM, intrinsic second-order phonon scattering is resolved as a broad band centered at  $540 \text{ cm}^{-1}$ , which is the only feature observed in the undoped reference sample.<sup>16</sup> The  $\text{C}_{\text{As}}$  LVM is superimposed on the high-frequency edge of this second-order phonon band. This edge arises from scattering by longitudinal-optical (LO) phonons at the center of the Brillouin zone.<sup>16</sup> Like scattering by the LVM produced by Si on the As site ( $\text{Si}_{\text{As}}$ ),<sup>10</sup> the  $\text{C}_{\text{As}}$  LVM Raman line is observed in configurations for which scattering described by a Raman tensor with  $\Gamma_{15}$  symmetry is allowed.

In infrared absorption the  $^{12}\text{C}_{\text{As}}$  LVM line shows, like that of the Be-on-Ga-site ( $^9\text{Be}_{\text{Ga}}$ ) acceptor,<sup>17</sup> a pronounced asymmetry in uncompensated material.<sup>8</sup> This asymmetric line shape has been explained by a Fano-type interference between the discrete vibrational mode and a continuum of electronic excitations.<sup>8,17</sup> Therefore one might have also expected such a Fano-type asymmetry for the  $\text{C}_{\text{As}}$  LVM Raman line. But, as for Raman scattering by the  $^9\text{Be}_{\text{Ga}}$  LVM, this is also not observed for the  $^{12}\text{C}_{\text{As}}$  LVM within the experimental noise limit. As dis-

cussed in Ref. 18, such an asymmetry might be expected to be weak for excitation with photon energies  $\geq 2.7$  eV.

Figure 2 shows the scattering intensity of the  $C_{As}$  LVM normalized to the intensity of the intrinsic second-order phonon scattering at  $540\text{ cm}^{-1}$  (Refs. 16 and 18) plotted versus the total carbon concentration  $[C]$  measured by SIMS. The data displayed are from samples 1–8. Those of sample 9 are omitted because in that sample, most probably, a considerable portion of the carbon is present as carbon-hydrogen pairs (see below).

From the relation<sup>18,19</sup>

$$I_{LVM} \sim [C_{As}] \sigma, \quad (1)$$

the LVM scattering intensity  $I_{LVM}$  is expected to increase linearly with the concentration of carbon atoms on arsenic sites,  $[C_{As}]$ , provided that the scattering cross section  $\sigma$  is constant. In Fig. 2 such a proportionality is indicated by the dashed line. The experimental data, however, are better described by the relation

$$I_{LVM} \sim [C]^{2/3}, \quad (2)$$

as shown by the solid line. As a possible explanation for this discrepancy, one has to keep in mind that the data in Fig. 2 are plotted versus the *total* carbon concentration  $[C]$ . However, the concentration of carbon atoms on arsenic sites  $[C_{As}]$ , which enters Eq. (1), may be, at least for the MBE-grown layers, only a fraction of  $[C]$ , with the other carbon atoms being incorporated as, e.g., interstitial atoms or clusters. Assuming that this fraction decreases with increasing  $[C]$  this may account at least for part of the discrepancy between Eq. (1) and the experimental data. Alternatively, one may think of a

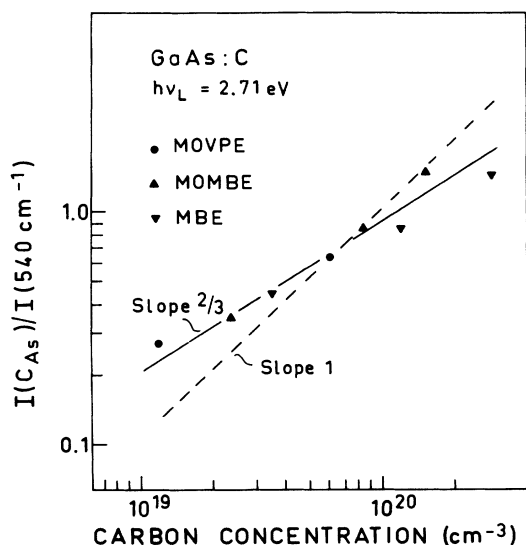


FIG. 2. Normalized Raman intensity of the  $^{12}C_{As}$  LVM  $[I(C_{As})/I(540\text{ cm}^{-1})]$  vs carbon concentration  $[C]$  (see Table I) for an incident-photon energy ( $h\nu_L$ ) of 2.71 eV. The samples were prepared by different growth techniques given in the figure. The dashed line indicates a proportionality between the LVM Raman intensity and the carbon concentration, and the solid line indicates a power law with an exponent of  $\frac{2}{3}$ .

concentration-dependent scattering cross section  $\sigma$  to account for this discrepancy. For Be-doped GaAs, however, a constant, concentration-independent cross section was found for excitation of the Raman spectra at 3.00 eV, which is in resonance with the GaAs  $E_1$ -band-gap energy.<sup>18</sup>

It is interesting to note that the LVM data for the MBE-grown layers indicate a  $C_{As}$  concentration significantly higher than the free-hole concentration (see Fig. 2 and Table I). This implies that the poor electrical activation in the MBE samples might be due to compensating defects.

A series of Raman spectra excited at different photon energies is shown in Fig. 3. The spectra were all recorded from a MOVPE-grown sample with a carbon concentration of  $1.8 \times 10^{20}\text{ cm}^{-3}$  (sample 9). The scattering configuration used was the same as for the spectra shown in Fig. 1. The spectrum excited at 2.71 eV is similar to those displayed in Fig. 1 showing the  $^{12}C_{As}$  LVM, except for the additional line labeled X at  $452\text{ cm}^{-1}$ . Tuning the incident-photon energy into resonance with the  $E_1$ -band-gap energy (3.00- and 3.05-eV excitation), the  $^{12}C_{As}$ -LVM line becomes masked by resonantly enhanced 2LO-phonon scattering.<sup>16</sup> The  $452\text{-cm}^{-1}$  line increases in relative intensity, with a pronounced maximum in scattering strength for excitation at 3.00 eV. This resonance behavior resembles that actually observed for LVM Raman scattering by Si on group-III lattice-site donors.<sup>20</sup>

Along with line X, a second additional Raman line is observed at  $2640\text{ cm}^{-1}$  (Fig. 4). This mode is superimposed on a photoluminescence background arising from

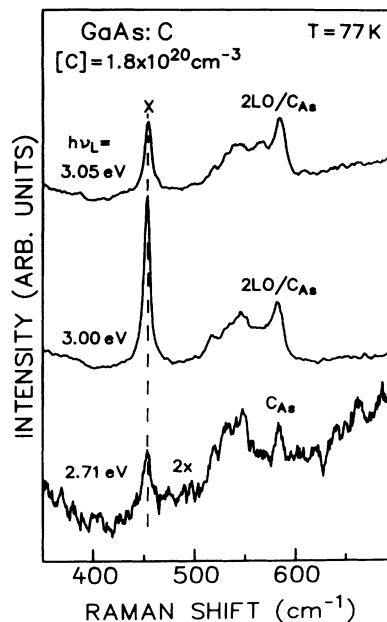


FIG. 3. Low-temperature Raman spectra of MOVPE-grown GaAs:C doped to a concentration of  $1.8 \times 10^{20}\text{ cm}^{-3}$  (sample 9 in Table I) excited at the different photon energies given in the figure. Spectral resolution was set to  $4\text{ cm}^{-1}$  for excitation at 2.71 eV and to  $5\text{ cm}^{-1}$  for 3.00- and 3.05-eV excitation.

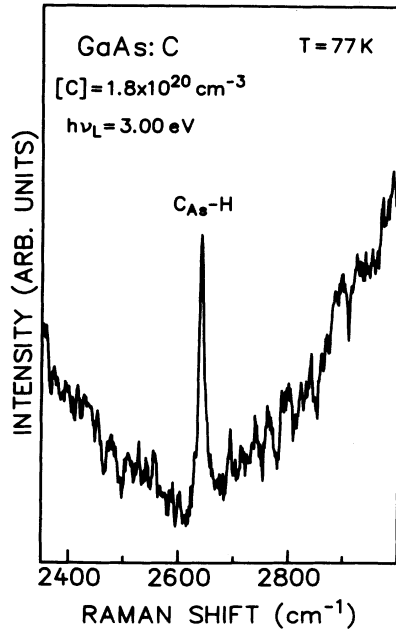


FIG. 4. Low-temperature Raman spectrum of MOVPE-grown GaAs:C with a dopant concentration of  $1.8 \times 10^{20} \text{ cm}^{-3}$  (sample 9 in Table I) excited at 3.00 eV. Spectral resolution was set to  $8 \text{ cm}^{-1}$ .

the recombination of nonthermalized electrons,<sup>21,22</sup> which is—by an order of magnitude—more intense than the Raman signal. The  $2640\text{-cm}^{-1}$  Raman line is also observed for excitation at 3.05 eV. For excitation at 2.71 eV, in contrast, this line can no longer be resolved against the luminescence background, which increases in intensity with decreasing photon energy.<sup>21,22</sup>

Recent infrared-absorption experiments revealed an absorption band at  $2636 \text{ cm}^{-1}$  arising from the stretch mode of the  $^{12}\text{C}_{\text{As}}\text{-H}$  pair both in intentionally hydrogen passivated, heavily-carbon-doped GaAs layers as well as in as-grown films prepared by MOMBE or MOVPE.<sup>7-9</sup> Thus, the  $2640\text{-cm}^{-1}$  Raman line observed in the present as-grown MOVPE layer can be assigned to this stretch mode. This assignment has been confirmed by Raman measurements on deuterated GaAs:C samples.<sup>23</sup> There is a slight shift in frequency relative to that reported for the absorption band, but at least part of that shift can be accounted for by the higher temperature of  $\approx 100 \text{ K}$  in the focus of the exciting laser in the present Raman experiment compared to that in the absorption experiments, which are usually carried out at liquid-He temperature. It has been established that the C-H stretch mode indeed shows an increase in frequency with increasing temperature.<sup>24</sup>

Having identified the presence of carbon-hydrogen pairs in the present MOVPE-grown layer, it is straightforward to assign the line X at  $452 \text{ cm}^{-1}$  to a carbon vibrational mode of these pairs. Infrared-absorption measurements revealed an absorption line at  $453 \text{ cm}^{-1}$  in hydrogen-passivated, carbon-doped material,<sup>8</sup> the strength of which was shown to be correlated with the carbon-hydrogen pair concentration.<sup>9</sup> According to re-

cent theory,<sup>25</sup> longitudinal and transverse modes are expected for the carbon-hydrogen pair, both lying on the low-frequency side of the LVM of the isolated carbon acceptor. These two modes have  $A_1$  and  $E$  symmetry, respectively.

To distinguish between the  $A_1$  and  $E$  modes, infrared absorption would require an external perturbing field created, e.g., by applying uniaxial stress. This situation, however, might be quite difficult when dealing with thin epitaxial layers. Here, Raman spectroscopy has the advantage of enabling one to discriminate between modes of different symmetry through the analysis of the polarization of the incident and scattered light. Figure 5 displays a series of Raman spectra recorded for different scattering configurations. These configurations were  $x(z',z')\bar{x}$ ,  $x(z,z)\bar{x}$ , and  $x(y,z)\bar{x}$ , where  $x, y, z$ , and  $z'$  denote [100], [010], [001], and [011] crystallographic directions. The  $452\text{-cm}^{-1}$  Raman line is strongest in intensity for configurations where the polarizations of the incident and scattered light are parallel to each other [ $x(z',z')\bar{x}$  and  $x(z,z)\bar{x}$ ], indicating that the vibrational mode causing this line has  $A_1$  symmetry<sup>15</sup> (note the scaling factor of 4 with which the lowest spectrum displayed in Fig. 5 [ $x(y,z)\bar{x}$ ] has been multiplied). This implies that the  $452\text{-cm}^{-1}$  (X) line arises from the longitudinal carbon mode of the carbon-hydrogen pair, which is in agreement with recent theoretical predictions.<sup>25</sup> In the frequency range of the  $^{12}\text{C}_{\text{As}}$  LVM for the  $x(y,z)\bar{x}$  configuration, only this carbon acceptor mode is observed, whereas in the  $x(z,z)\bar{x}$  configuration, only 2LO-phonon scattering is allowed. In the  $x(z',z')\bar{x}$  configuration both the LVM

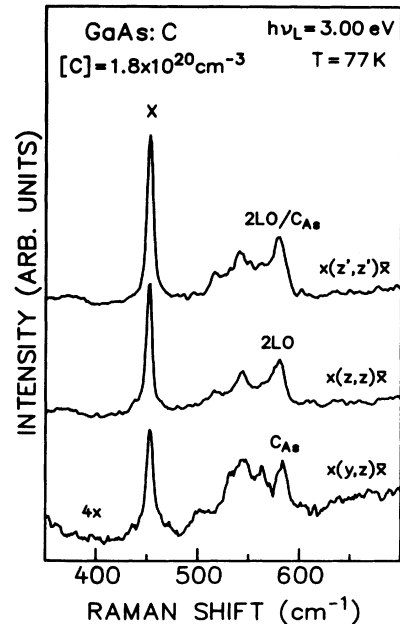


FIG. 5. Low-temperature Raman spectra of MOVPE-grown GaAs:C with a dopant concentration of  $1.8 \times 10^{20} \text{ cm}^{-3}$  (sample 9 in Table I). The spectra were excited at 3.00 eV and recorded for different scattering configurations indicated in the figure. Spectral resolution was set to  $5 \text{ cm}^{-1}$ .

and the 2LO peak are superimposed, with 2LO-phonon scattering being dominant.

In infrared absorption an additional carbon-related line has been observed at  $563\text{ cm}^{-1}$ , the origin of which is not yet clear.<sup>8,9</sup> It may arise either from the carbon on the Ga-site ( $C_{\text{Ga}}$ ) donor, or the transverse carbon mode of the hydrogen pair, or alternatively from carbon-carbon pairs.<sup>8,9</sup> We cannot resolve this line in the present Raman spectra, possibly because it would be superimposed on the comparatively strong second-order Raman signal centered at  $\approx 540\text{ cm}^{-1}$ .

The dependence of the strength of the  $452\text{-cm}^{-1}$  ( $X$ ) Raman line on carbon concentration  $[C]$  is illustrated in Fig. 6 for the present set of MOVPE-grown layers (samples 7–9). For a carbon concentration of  $1.2 \times 10^{19}\text{ cm}^{-3}$  the  $X$  line is below our detection limit, whereas for  $[C] = 6 \times 10^{19}\text{ cm}^{-3}$  it is just resolved and it is by far the strongest for the most heavily doped layer with  $[C] = 1.8 \times 10^{20}\text{ cm}^{-3}$ . The strength of the  $X$  line is independent of depth underneath the sample surface, as it has been checked for the most heavily doped sample by successively etching away the epitaxial layer. Based on the correlation between the  $452\text{-cm}^{-1}$  mode and the carbon-hydrogen stretch mode presented in Ref. 9, we can take the scattering intensity of the  $X$  line as a semi-quantitative measure for the carbon-hydrogen pair concentration. This implies that the formation of measurable concentrations of carbon-hydrogen pairs takes place for the present MOVPE technique at carbon concentrations greater than  $5 \times 10^{19}\text{ cm}^{-3}$ . Here we have to keep in mind that the carbon-doping level is adjusted by growth parameters such as the growth temperature (see Sec. II). The onset of hydrogen incorporation coincides with a reduction in doping efficiency, which is close to unity up to a carbon concentration of  $6 \times 10^{19}\text{ cm}^{-3}$  and drops to  $\frac{2}{3}$  for  $[C] = 1.8 \times 10^{20}\text{ cm}^{-3}$  (see samples 7–9 in Table I). However, it would require a calibration of the Raman-scattering intensity, which is not available at present, to quantify the concentration of carbon-hydrogen pairs and, consequently, to clarify whether the formation of carbon-hydrogen pairs does account quantitatively for this reduction in doping efficiency.

It is interesting to note that we do not observe a hydrogen-related LVM in the present MOMBE layers, which is in accord with the results reported by Woodhouse *et al.*<sup>8</sup> However, the first observation of hydrogen-related modes in as-grown carbon-doped GaAs layers was in MOMBE-grown samples.<sup>7</sup> A possible reason for these different findings could be the specific growth conditions employed and, in particular, the hydrogen background pressure.

#### IV. CONCLUSIONS

We have presented Raman LVM spectra of heavily-carbon-doped GaAs epitaxial layers grown by MBE,

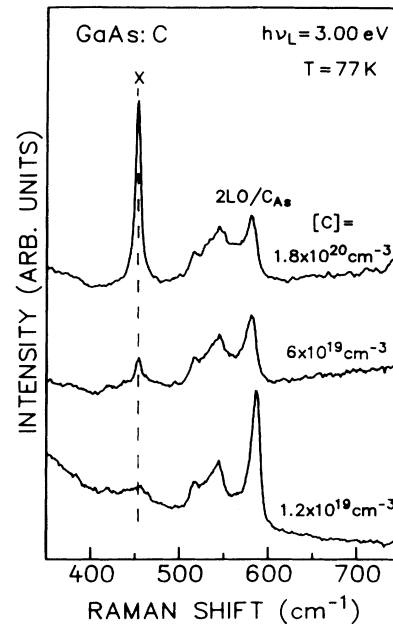


FIG. 6. Low-temperature Raman spectra of MOVPE-grown GaAs:C with different dopant concentrations (see Table I). The spectra were excited at 3.00 eV and recorded with a spectral resolution of  $5\text{ cm}^{-1}$ .

MOMBE, and MOVPE. The scattering intensity of the carbon-acceptor ( $^{12}\text{C}_{\text{As}}$ ) LVM has been correlated with the total carbon concentration in the layer measured by SIMS. A comparison of the SIMS data with Hall measurements shows a reasonable electrical activation of the carbon dopant for the MOMBE- and MOVPE-grown layers. Raman spectra from heavily carbon-doped MOVPE-grown layers show two additional lines assigned to the stretch mode and the longitudinal carbon mode of carbon-hydrogen pairs. The latter assignment is based on the analysis of polarization-selection rules. Scattering by the longitudinal carbon mode was found to be strongly resonant for incident-photon energies matching the  $E_1$ -band-gap energy of GaAs.

#### ACKNOWLEDGMENTS

We would like to thank K. Winkler, T. Fuchs, and F. Pohl for valuable technical assistance, P. Koidl and W. Pletschen for helpful discussions, and H. S. Rupprecht for continuing support of the work at the Fraunhofer-Institut. Thanks are also due R. C. Newman for valuable discussions and for communicating results prior to publication.

<sup>1</sup>T. F. Kuech, M. A. Tischler, P. J. Wang, G. Scilla, R. Potemski, and F. Cardone, *Appl. Phys. Lett.* **53**, 1317 (1988).

<sup>2</sup>K. Saito, E. Tokumitsu, T. Akatsuka, M. Miyauchi, T. Yamada, M. Konagai, and K. Takahashi, *J. Appl. Phys.* **64**, 3975

(1988).

<sup>3</sup>C. R. Abernathy, S. J. Pearton, R. Caruso, F. Ren, and J. Kovalchik, *Appl. Phys. Lett.* **55**, 1750 (1989).

<sup>4</sup>M. Konagai, T. Yamada, T. Akatsuka, K. Saito, E. Tokumitsu,

- and K. Takahashi, *J. Cryst. Growth* **98**, 167 (1989).
- <sup>5</sup>T. J. de Lyon, J. M. Woodall, M. S. Goorsky, and P. D. Kirchner, *Appl. Phys. Lett.* **56**, 1040 (1990).
- <sup>6</sup>See, e.g., R. C. Newman, *Mater. Res. Soc. Symp. Proc.* **46**, 459 (1985), and references therein.
- <sup>7</sup>D. M. Kozuch, M. Stavola, S. J. Pearton, C. R. Abernathy, and J. Lopata, *Appl. Phys. Lett.* **57**, 2561 (1990).
- <sup>8</sup>K. Woodhouse, R. C. Newman, T. J. de Lyon, J. M. Woodall, G. J. Scilla, and F. Cardone, *Semicond. Sci. Technol.* **6**, 330 (1991).
- <sup>9</sup>K. Woodhouse, R. C. Newman, R. Nicklin, R. R. Bradley, and M. J. L. Sangster, *J. Cryst. Growth* (to be published); K. Woodhouse, R. C. Newman, R. Nicklin, and R. R. Bradley (unpublished).
- <sup>10</sup>See, e.g., J. Wagner, *Mater. Sci. Forum* **65-66**, 1 (1990), and references therein.
- <sup>11</sup>J. Wagner, in *Light Scattering in Semiconductor Structures and Superlattices*, NATO Advanced Research Workshop Series (Plenum, New York, in press).
- <sup>12</sup>SUKO 35 carbon effusion cell (MBE-Komponenten GmbH, D-8047 Karlsfeld, FRG).
- <sup>13</sup>G. Neumann, Th. Lauterbach, M. Maier, and K. H. Bachem, *Inst. Phys. Conf. Ser.* **112**, 167 (1990).
- <sup>14</sup>M. Cardona and G. Harbeke, *J. Appl. Phys.* **34**, 813 (1962).
- <sup>15</sup>See, e.g., M. Cardona, in *“Light Scattering in Solids II”*, edited by M. Cardona and G. Gütherodt (Springer, New York, 1982), p. 19.
- <sup>16</sup>R. Trommer and M. Cardona, *Phys. Rev. B* **17**, 1865 (1978).
- <sup>17</sup>R. Murray, R. C. Newman, R. S. Leigh, R. B. Beall, J. J. Harris, M. R. Brozel, A. Mohades-Kassei, and M. Goulding, *Semicond. Sci. Technol.* **4**, 423 (1989).
- <sup>18</sup>J. Wagner, M. Maier, R. Murray, R. C. Newman, R. B. Beall, and J. J. Harris, *J. Appl. Phys.* **69**, 971 (1991).
- <sup>19</sup>J. Wagner, *Appl. Surf. Sci.* **50**, 79 (1991).
- <sup>20</sup>J. Wagner, P. Koidl, and R. C. Newman, *Appl. Phys. Lett.* **59**, 1729 (1991).
- <sup>21</sup>B. J. Aitchison, N. M. Haegel, C. R. Abernathy, and S. J. Pearton, *Appl. Phys. Lett.* **56**, 1154 (1990).
- <sup>22</sup>J. Sapriel, J. Chavignon, F. Alexandre, R. Azoulay, B. Sermage, K. Rao, and M. Voos, *Solid State Commun.* **79**, 543 (1991).
- <sup>23</sup>J. Wagner, M. Ashwin, R. C. Newman, K. Woodhouse, R. Nicklin, and R. R. Bradley (unpublished).
- <sup>24</sup>B. Clerjoud, D. Cote, F. Gendron, W. S. Hahn, M. Krause, C. Porte, and W. Ulrici, *Mater. Sci. Forum* **83-87**, 563 (1992).
- <sup>25</sup>R. Jones and S. Öberg, *Phys. Rev. B* **44**, 3673 (1991).